A Study on Model-based Optimization of Vaccination Strategies against Epidemic Virus Spread

Zonglin Liu, Muhammed Omayrat and Olaf Stursberg
Control and System Theory, Dept. of Electrical Engineering and Computer Science, University of Kassel, Germany

Keywords: Epidemic Modeling, Markov Process, Infection Control, Optimal Control, Biomedical Systems.

Abstract: This paper aims at applying optimal control to investigate different vaccination strategies against the epidemic spread of viral diseases. Background of the study is the situation in the first half of 2021, when many countries started their vaccination procedures against the COVID-19 disease, but suffered from shortages of vaccines, such that the efficient distribution of the available amount of vaccine turned out to be crucial to mitigate the pandemic. The paper first suggests an extended version of a known model of virus spread in order include the vaccination process. Based on this model, the formulation and solution of optimization problems is used to determine how available vaccine should be distributed over different age-groups of the population to minimize virus spread. Effectiveness of the obtained strategies compared to standard ones is demonstrated in simulations.

1 INTRODUCTION

In 2020, the outbreak and rapid spread of COVID-19 affected the life of almost everyone on the planet. Facing high infection and mortality rates, as well as the absence of efficient treatment to patients, strict intervention policies (such as lock-down of cities and restricting social life) were deployed by the governments to control the spread of the virus. Effectiveness of these policies, however, were barely satisfactory in many countries for several months with respect to the daily number of active cases and the number of fatalities. The successful development of vaccines in the beginning of 2021, led to the hope that life may return to normal rather quickly, but limited production capacities of the vaccines led to the situation that only a small shares of the population could be vaccinated during the first half of 2021. Thus, the question of how to control the vaccination process subject to the given capacity constraints turned out to be crucial to mitigate the pandemic – and this, of course, is a central question to any future pandemic virus disease.

Before the outbreak of COVID-19, different vaccination strategies had been proposed in literature, including the uniform strategy, see (Pastor-Satorras et al., 2003), the targeted strategy, see (Liu et al., 2003), the random strategy, see (Zanette and Kuperman, 2002), and the acquaintance strategy, see (Cohen et al., 2003). (Preciado et al., 2013) considered optimal vaccination strategies by taking the vaccination cost into account, using a Susceptible-Infected-Susceptible (SIS) epidemic model (see (Kermack and McKendrick, 1932), (Ganesh et al., 2005)) for describing the virus spread. (Peng et al., 2010) followed a similar pattern to develop an optimal vaccination strategy, but considered additional constraints in optimization of the SIS model. (Wan et al., 2007) focused on the case that the vaccination resources are limited, and they exploited the topological structure of the network to eliminate the virus. The resulting vaccination strategy was then tested on a model for the SARS transmission in 2003. The work by (Gourdin et al., 2011) investigated how to efficiently distribute available medicine to minimize the overall infection. Unlike vaccines, which reduce the individual infection rate, the medicine in the latter work is assumed to increase the individual curing rate.

Most of these strategies are based on the SIS model, in which only two states of the individuals are modelled, namely, to be susceptible for the virus or being infected. Experiences from COVID-19 have shown, however, that aspects like the questions of whether an infected person has symptoms or not, or of whether she/he can be tested in time (and is isolated before infecting others) are decisive for the evolution of the virus spread. Accordingly, the determination of an optimal (or at least good) vaccination strategy must also take these aspects into account. In addition,

Liu, Z., Omayrat, M. and Stursberg, O.
A Study on Model-based Optimization of Vaccination Strategies against Epidemic Virus Spread.
DOI: 10.5220/0010604006300637
In *Proceedings of the 18th International Conference on Informatics in Control, Automation and Robotics (ICINCO 2021)*, pages 630-637
ISBN: 978-989-758-522-7

most of the work mentioned above also assumed that the population can be modeled homogeneously in the sense that the same rates of infections, courses of developing symptoms or being cured apply to anyone. Observations for the first year of COVID-19 clearly showed differences, however, with respect to senior members of the population have significantly higher mortality rates and lower curing rates than younger generations.

To capture such characteristics, this paper first reviews in Sec. 2 recent work on COVID-19 modeling, and then extends the model proposed in (Giordano et al., 2020) by including the vaccination process in Sec. 2. Note that the selected model was proposed to account for the course of the COVID-19 pandemic in Italy and it includes already more states than the SIS-model, but does not account for vaccination. Based on the extended model, optimal control problems are formulated and solved in order to determine optimal vaccination strategies in Sec. 3. The solution takes into account different age groups of the population and heterogeneity with respect to infection and curing rates, as well as different contact situations and limitations of the amount of available vaccines. In Sec. 4, the computed strategies are simulated exemplarily for a mid-size city and compared to alternative strategies, before Sec. 5 concludes the paper.

2 THE EPIDEMIC MODEL

Most literature on epidemic modeling uses the SIS model to describe the spread of a virus. In this rather simple model, only two states of any individual, susceptible and infected, are considered. After the first outbreak of the COVID-19 pandemic, different groups have invested effort into adapting the SIS model to the characteristics of this disease: The work in (Della et al., 2020) considered the networked structure of different regions in Italy and extended the SIS model with four more states, i.e., quarantined, hospitalized, recovered, and deceased. In the work of (Ndaïrou et al., 2021), even more COVID-19 related states are included and the influence of superspreading individuals are studied. In (Chaturvedi and Chakravarty, 2021), the authors applied the SIR model (with R for recovered) to provide a predictive analysis of when the pandemic can be ended with the help of vaccination. Among these efforts, the so-called SIDARTHE model, which was proposed in (Giordano et al., 2020) and is shown by the part marked in black in Fig. 1, has been widely adopted in different work, see (Köhler et al., 2020; López and Rodó, 2020).

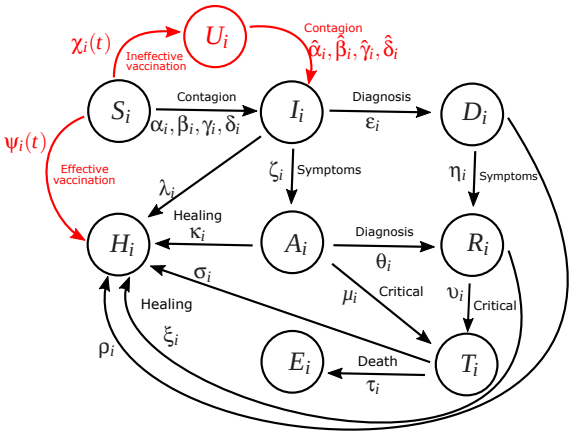

Figure 1: The states and transitions in black represent the original SIDARTHE model, while the parts in red are newly added to model the vaccination process, as well as are the indices i to model different groups of persons.

The SIDARTHE model, distinguishes the following health status: being susceptible (S_i), infected (I_i), diagnosed (D_i), ailing (A_i), recognized (R_i), threatened (T_i), healed (H_i), and extinct (E_i). The corresponding states represent the percentage of persons of a given population with the corresponding health status, and the changes of these percentages is modeled stochastically by a continuous-time Markov process. The first extension of this model compared to earlier papers is to refer to a set of n groups of persons, where the index $i \in N = \{1, \cdots, n\}$ refers to one these groups. This extension will allow later to refer to a certain age-group of the population. The sum of the percentages over the discrete states of the Markov process for a single group i is always one.

Note that, although the SIDARTHE model can well represent the development of the pandemic, it was proposed in March 2020, when vaccines were still not yet in sight. This can be noticed from the black part in Fig. 1, since the health status cannot transition directly from S_i to H_i without being infected. Accordingly, the SIDARTHE model is extended in this paper also to contain the vaccination process (see the red part in Fig. 1). This includes the addition of one state U_i referring to the percentage of people in group i, for whom the vaccine is ineffective. In addition, three new transitions are also assigned, namely, from S_i to H_i, from S_i to U_i, and from U_i to I_i. In order to model the evolution of the probability distribution over the discrete states for group $i \in N$, the following nonlinear dynamics is selected:

$$\dot{S}_i(t) = -S_i(t) \sum_{j \in N} W_{ij} (\alpha_i I_j(t) + \beta_i D_j(t) + \gamma_i A_j(t) + \delta_i R_j(t)) - (\chi_i(t) + \psi_i(t)) S_i(t) \quad (1)$$

$$\dot{U}_i(t) = -U_i(t)\sum_{j\in N} W_{ij}(\hat{\alpha}_i I_j(t) + \hat{\beta}_i D_j(t) + \hat{\gamma}_i A_j(t) + \hat{\delta}_i R_j(t)) + \chi_i(t) S_i(t) \quad (2)$$

$$\dot{I}_i(t) = S_i(t)\sum_{j\in N} W_{ij}(\alpha_i I_j(t) + \beta_i D_j(t) + \gamma_i A_j(t) + \delta_i R_j(t)) - (\varepsilon_i + \zeta_i + \lambda_i) I_i(t) + U_i(t)\sum_{j\in N} W_{ij}(\hat{\alpha}_i I_j(t) + \hat{\beta}_i D_j(t) + \hat{\gamma}_i A_j(t) + \hat{\delta}_i R_j(t)) \quad (3)$$

$$\dot{D}_i(t) = \varepsilon_i I_i(t) - (\eta_i + \rho_i) D_i(t) \quad (4)$$

$$\dot{A}_i(t) = \zeta_i I_i(t) - (\theta_i + \mu_i + \kappa_i) A_i(t) \quad (5)$$

$$\dot{R}_i(t) = \eta_i D_i(t) + \theta_i A_i(t) - (\upsilon_i + \xi_i) R_i(t) \quad (6)$$

$$\dot{T}_i(t) = \mu_i A_i(t) + \upsilon_i R_i(t) - (\sigma_i + \tau_i) T_i(t) \quad (7)$$

$$\dot{H}_i(t) = \lambda_i I_i(t) + \rho_i D_i(t) + \kappa_i A_i(t) + \xi_i R_i(t) + \sigma_i T_i(t) + \psi_i(t) S_i(t) \quad (8)$$

$$\dot{E}_i(t) = \tau_i T_i(t) \quad (9)$$

For consistent initialization of the model in an initial time t_0, it is required for any $i \in N$ that the sum of all states is one. Note that the model also satisfies $\dot{S}_i(t) + \dot{U}_i(t) + \dot{I}_i(t) + \dot{D}_i(t) + \dot{A}_i(t) + \dot{R}_i(t) + \dot{T}_i(t) + \dot{H}_i(t) + \dot{E}_i(t) = 0$ at any time t for any choice of parameters. These are denoted by α_i, β_i, γ_i, δ_i, ε_i, ζ_i, λ_i, η_i, θ_i, υ_i, ξ_i, τ_i, ρ_i, σ_i, μ_i, and model the transition rates in between the pairs of corresponding states. The different contagion parameters $\alpha_i, \beta_i, \gamma_i, \delta_i$ in the transition from S_i to I_i are due to contacts between a susceptible person and an infected, a diagnosed, an ailing, or a recognized person according to the original paper in (Giordano et al., 2020). These parameters together with other transitions rates in Fig. 1 are assumed to be known[1], but differ among the different groups $i \in N$. In detail and compared to the original SIDARTHE model, the new model here covers the following effects in addition: 1.) a successful vaccination step (transition from S_i to H_i) with rate $\psi_i(t) \in \mathbb{R}^{\geq 0}$. The rates $\psi_i(t)$ will be used as inputs determining the vaccination strategy to be optimized in the coming section; 2.) an ineffective vaccination step (from S_i to U_i) with rate $\chi_i(t) \in \mathbb{R}^{\geq 0}$, where $\chi_i(t)$ is assumed to be proportional to $\psi_i(t)$, i.e., $\chi_i(t) = q \cdot \psi_i(t)$, $q \in \mathbb{R}^{>0}$; 3.) an infection step (from U_i to I_i) with respective contagion parameters $\hat{\alpha}_i$, $\hat{\beta}_i$, $\hat{\gamma}_i$, and $\hat{\delta}_i$. Note that the labeling of this transition with four rates refers to the shares that a person in state U_i gets infected by contact with a person in state I_i, D_i, A_i or R_i respectively (the same principle underlies the assignment of four parameters to the transition from S_i to I_i). Note further that the contagion parameters assigned to $U_i \to I_i$ are different from those assigned to $S_i \to I_i$ to account for the possibility that a vaccinated person, which is unaware of the fact that the vaccination was not successful, will likely follow relaxed contact patterns, compared to persons that still wait to be vaccinated.

In order refer to the above model in brief, let it be denoted by:

$$\dot{x}_i(t) = f(x_i(t), \psi_i(t)),\ x_i(t_0) = x_{i,0} \quad (10)$$

with state vector $x_i(t) := (S_i(t), U_i(t), I_i(t), D_i(t), A_i(t), R_i(t), T_i(t), H_i(t), E_i(t))$, and the initial state $x_{i,0}$. Furthermore, the model aims at considering the spread of the virus across different age groups of the population. In order to formalize the contacts between different age groups, and thus the possibility that infections occur across the groups, an undirected graph $G = \{N, E\}$ is set up. In here, the set N of nodes models the different age groups, with indices $i \in N$ as before. The set E of undirected edges models the contact between a pair of groups. To an edge $e_{i,j} \in E$ between the groups with indices i and j, a positive weight $W_{ij} \in \mathbb{R}^{>0}$ is assigned, representing that infections in group j can affect the infection in group i (and vice versa), see also (1) - (3) in the model. More precisely, a weight W_{ij} models the average share of time that a person from group i spends with a person from group j. Accordingly, a self-loop transition with weight W_{ii} is introduced for any node, and the matrix $W \in \mathbb{R}^{n\times n}$ is chosen as doubly stochastic matrix, i.e., $\sum_{j\in N} W_{ij} = 1$ for all $i \in N$, and $\sum_{i\in N} W_{ij} = 1$ for all $j \in N$.

Note that the model in the present form does not explicitly account for the necessity that two (or more) shots of vaccine may be necessary to get from state S_i to H_i. This could be included by introducing intermediate state in between $S_i \to H_i$ and $S_i \to U_i$, but is omitted here to not overload the model.

3 DETERMINATION OF OPTIMIZED VACCINATION STRATEGIES

Based on the model introduced before, this section proposes to determine vaccination strategies for different age-groups of the population based on optimal control principles. The underlying assumption is that there is a shortage of available vaccine (as was true for the COVID-19 pandemic in the first half year after developing the vaccine). This, together with the observation that the infection has, on average, more severe

[1] In practice, one can only estimate these parameters, leading to model uncertainty. In order to consider e.g. parameter intervals, extensions to techniques of robust predictive control could be employed, see (Campo and Morari, 1987), but this is outside of the scope of the present paper.

effects the older the infected person is, motivates to divide the population into n groups according to their age. For any age-group with index $i \in N = \{1, \cdots, n\}$, let its share of the total population be denoted by v_i, and $\sum_{i \in N} v_i = 1$. The vaccination of different age groups (represented in the model from Sec. 2 by the rates $\psi_i(t)$ and $\chi_i(t)$) as well as contacts between age groups (modelled by the weights W_{ij}) can be expected to have significant impact on the evolution of the epidemic.

3.1 Optimization Objectives and Constraints

In order to set up the optimal control formulation, first let an initial time t_0 be given as well as a time interval $[t_0, t_0 + H]$, where H is the number of days over which the vaccine is distributed. Assume that the vaccination strategy can only be adjusted every T days of the horizon, leading to totally $\frac{H}{T}$ decision steps. Let $k \in \{0, 1, \cdots, \frac{H}{T} - 1\}$ index these steps. Once the strategy is determined for k it is held constant for the coming T days. Accordingly, the vaccination rate applied to an age-group $i \in N$ on the interval $[k \cdot T, (k+1) \cdot T[$ is referred to by $\psi_{i,k}$. The maximum amount of vaccine available for step k over all groups i is denoted by $\Psi_{max,k}$, leading to the following constraint:

$$\sum_{i \in N} \mathcal{P} \cdot v_i \cdot (\psi_{i,k} + \chi_{i,k}) \leq \Psi_{max,k}, \tag{11}$$

with a population size $\mathcal{P}$, and $\mathcal{P} \cdot v_i$ representing the size of age-group i. Corresponding to the relation between $\chi_i(t)$ and $\psi_i(t)$ as mentioned in Sec. 2, it follows that: $\chi_{i,k} := q \cdot \psi_{i,k}$.

Given the constraint (11), the task is now to optimize the vaccination strategy $\psi := (\psi_0, \psi_1, \ldots, \psi_{\frac{H}{T}-1})$ with $\psi_k = (\psi_{1,k}, \ldots, \psi_{n,k})^T$ for all age-groups in all decision steps, in order to minimize the infected share of the population (i.e., all persons assigned to the states I_i, D_i, A_i, R_i, T_i in Fig. 1), as well as the death cases (referring to the state E_i). To consider, in addition, the vaccination costs, an additional term can be introduced, leading to the following cost function:

$$\begin{aligned} J(\psi) := \sum_{i \in N} \Bigg(\int_{t_0}^{t_0+H} & \mathcal{P} v_i (c_1 \cdot (I_i(t) + D_i(t) + A_i(t) \\ & + R_i(t) + T_i(t)) + c_2 \cdot E_i(t))\, dt \\ & + c_3 \cdot \sum_{k \in \{0, \cdots, \frac{H}{T}-1\}} \psi_{i,k} \Bigg). \end{aligned} \tag{12}$$

The parameters c_1, c_2 and c_3 (all positive) denote appropriate weights of the terms of the cost function.

Note that $J(\psi)$ may be extended to additional cost terms to account, e.g., for costs of testing. Likewise, additional constraints, as limitations in available staff for vaccination could be considered.

3.2 The Optimization Problem

In order to determine an optimized vaccination strategy, denoted by ψ^*, the aforementioned objectives and constraints together with the model (10) are cast into the following optimization problem:

Problem 1.

$$\min_{\psi} J(\psi) \tag{13}$$

s.t. for all $i \in N$ *and given* G :

$x_i(t_0) = x_{i,0},\ t \in [t_0, t_0 + H]$,

dynamics (10),

$$\text{for all } k \in \{0, \ldots, \frac{H}{T} - 1\} : \tag{14}$$

$$\psi_{i,k} \geq 0, \tag{15}$$

$$\sum_{i \in N} \mathcal{P} \cdot v_i \cdot (1+q) \psi_{i,k} \leq \Psi_{max,k}. \tag{16}$$

The optimized strategy ψ^* is then determined by solving this nonlinear continuous-time optimization problem. The constraint (14) is a local constraint of group i, while (16) determines a coupling constraint. The dynamics of the groups is also coupled through the matrix W affecting (1) - (3).

To solve Problem 1, one can apply, e.g., techniques of multiple shooting, see e.g. (Bock et al., 2000), which casts the original problem into a finite dimensional nonlinear programming problem by parameterizing the input and state space. One should note, however, that one can only hope to determine a sub-optimal strategy for the given non-convex problem (this is why it is referred to an optimized strategy, rather than the optimal one).

4 SIMULATION

To illustrate the computation of optimized vaccination strategies and to discuss a number of effects, consider a midsize city with a population of $\mathcal{P} = 200,000$. According to a statistics of distribution of the population over the age groups $i \in N$ (in Germany for 2021), consider the following values for the city:

Table 1: Distribution over age groups.

Age	**0-19**	**20-39**	**40-59**	**60-79**	**80+**
v_i	18.5%	24.6%	28.8%	21.6%	6.5%

Table 2: Contacts between different age-groups during the epidemic.

Age	0-19	20-39	40-59	60-79	80+
0-19	31%	34%	25%	8%	2%
20-39	34%	45%	15%	5%	1%
40-59	25%	15%	30%	20%	10%
60-79	8%	5%	20%	50%	17%
80+	2%	1%	10%	17%	70%

The estimated average time (in percentage) persons of one group spend with those of another is listed in Table 2, representing the entries of matrix W. Note that Table 2 also reflects certain intervention policies deployed in certain phases in Germany, such as that visiting nursing homes was forbidden (such that the most senior group had to spent most of their time with its own), while schools were open during that phase. The parameters contained in the dynamics (1) - (9) are chosen similar to (Giordano et al., 2020), except for the following:

- The contagion parameters $\hat{\alpha}_i, \hat{\gamma}_i$ for the transition from $U_i \to I_i$ are larger than for $S_i \to I_i$. This aims at reflecting the effect that people are less cautious to the virus after being vaccinated, although the vaccination may be ineffective.
- Effectiveness of the vaccine is assumed to be 90% for all age-groups[2], i.e., $\chi_i := 0.11\psi_i$, $i \in N$.

The initial states for t_0 are chosen according to the pandemic situation of the city at the end of 2020. The considered horizon is $H = 90$ days, and the vaccination strategy can be changed every $T = 30$ days (thus, in total 3 decision steps). The weights in J satisfy $c_2 > c_1 \gg c_3$, i.e., the main goal is to reduce the overall number of casualties, while the vaccine costs can be neglected.

4.1 Uniform Vaccination Strategy

Before the optimized strategy is tested, a uniform vaccination strategy is first simulated: When assuming that the availability of the vaccine is constant in all decision steps, i.e., $\Psi_{max,k} := \Psi_{max}$, $\forall k \in \{0,1,2\}$, the $\psi_{i,k}$ in the uniform vaccination strategy takes a value of: $\psi_{i,k} := \frac{\Psi_{max}}{\mathcal{P}\cdot(1+q)}$ for all $i \in N$. The outcome by adopting this strategy is illustrated in Fig. 2 and 3. Obviously, most of the casualties occur in the senior groups **60 - 79** and **80+**, although the number of infections (over the states infected (I_i), diagnosed (D_i), ailing (A_i), recognized (R_i) and threatened (T_i)) in these groups are not the highest. This is mainly due to the high mortality rate of the two groups.

[2]This may be extended to considering different effectiveness rates of the vaccine for different age-groups, or to different rates for different types of vaccines.

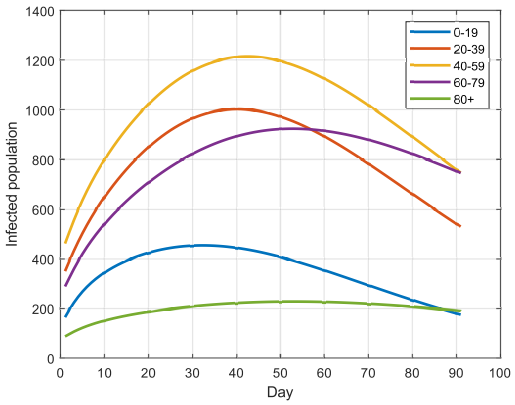

Figure 2: Number of infections when applying the uniform strategy over $H = 90$ days.

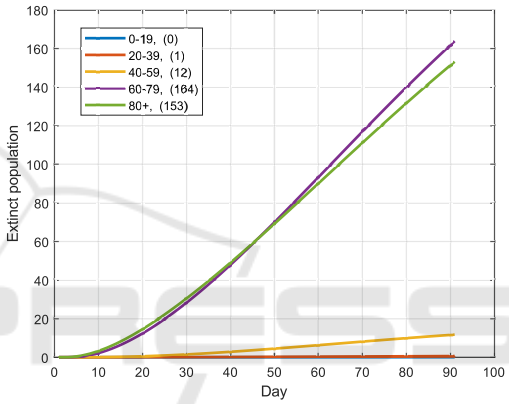

Figure 3: Casualties for each age group with the uniform strategy at the end of the 90 days.

4.2 Optimized Vaccination Strategy

In the second test, the Problem 1 is solved to determine the optimal vaccination strategy. The resulting $\psi^*_{i,k}$ for each group is shown in Fig. 4. By adopting this strategy, the evolution of the infections and casualties are illustrated in Fig. 5 and 6. Compared to the uniform strategy, more infected cases occur in the groups **20 - 39** and **40 - 59**, while less in the groups **60 - 79** and **80+**. The casualties for the two senior groups, however, is significantly reduced by adopting the optimized strategy, and this also leads to a decrease of the total number of casualties from 329 to 174, see Fig. 7 and 8.

The optimized strategy is further compared to the popular strategy of first vaccinating the older generations, see Fig. 9 and 10. In this strategy, all available vaccine is first provided to the group **80+** in the steps

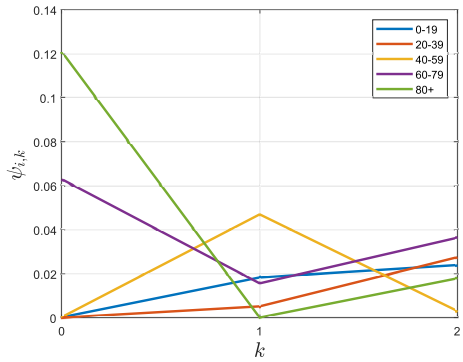

Figure 4: The optimized vaccination strategy from Problem 1: in $k = 0$, the complete available vaccine is distributed to the groups **60 - 79** and **80+**; in $k = 1$, most of the vaccine is distributed to the group **40 - 59**, **60 - 79** and **0 - 19**; in the last step $k = 2$, the vaccine is distributed to all groups besides the group **40 - 59**.

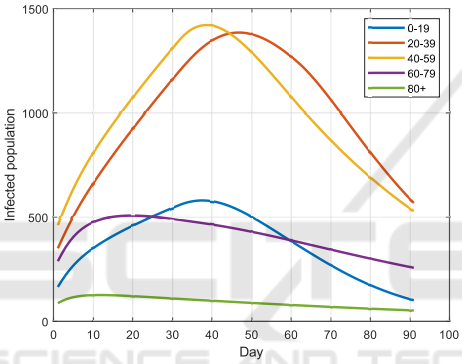

Figure 5: Infections with the optimized strategy.

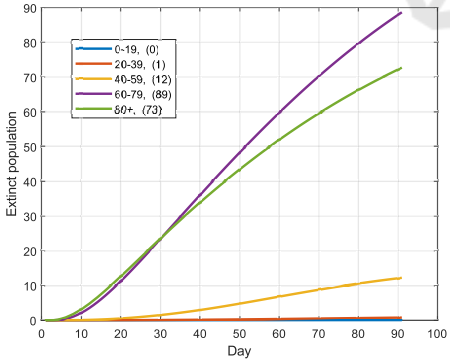

Figure 6: Casualties with the optimized strategy.

$k = 0$ and $k = 1$, and then to the group **60 - 79** for $k = 2$. One can notice, however, that only the number of casualties in the group **80+** is slightly reduced compared to the uniform strategy, while much more occur in the group **60 - 79**. This is due to the larger size of the latter group than the **80+** group, and to the more frequent contacts of this group with younger persons.

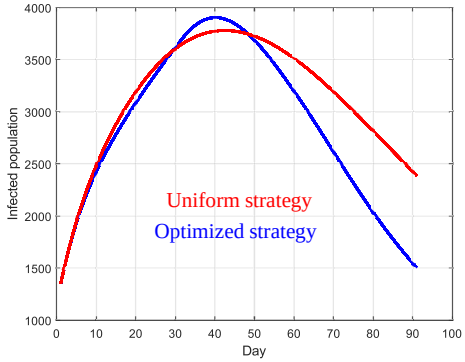

Figure 7: Infections over all age-groups by adopting the uniform vaccination strategy and the optimized one.

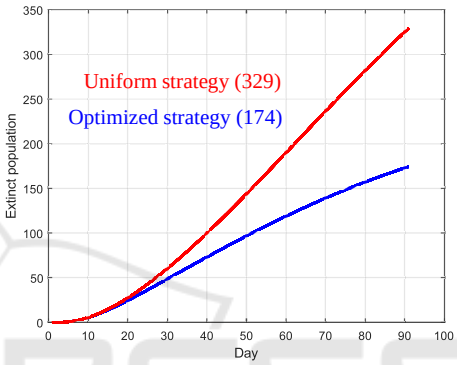

Figure 8: Casualties over all age-groups by adopting the uniform vaccination strategy and the optimized one.

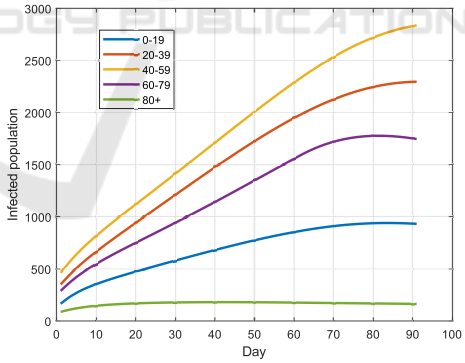

Figure 9: Infections when applying the older-first strategy.

The immunity of the group **60 - 79** is, however, only slightly better than for the **80+** group, but much worse than for the junior groups. Accordingly, the group **60 - 79** should not be ignored in the first step of the vaccination process based on the simulation results.

4.3 Increasing Availability of Vaccine

In the third test, it is assumed that more vaccine can be provided over time, i.e., $\Psi_{max,k} := 2^k \cdot \Psi_{max}$,

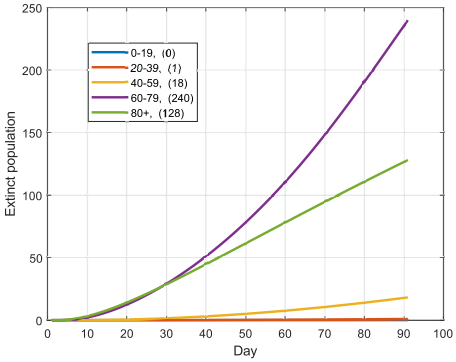

Figure 10: Casualties when applying the older-first strategy.

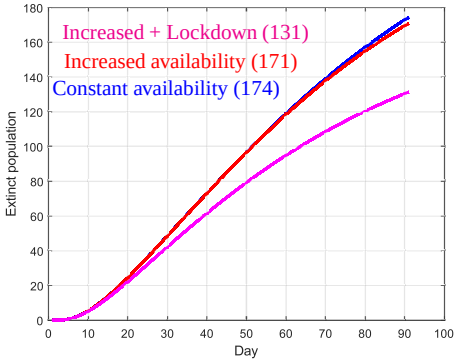

Figure 12: Casualties by applying the strategies in Fig. 11.

$k \in \{0,1,2\}$. The new outcome from solving Problem 1 is illustrated in Fig. 11 and 12. Compared with the last test, in which the available amount vaccine is constant over time, the total number of casualties has been barely reduced, but a decrease of the total number of infections can be observed after 30 days. In another test with $\Psi_{max,k} := 2^k \cdot \Psi_{max}$, the infections rates for the transitions $S_i \to I_i$ and $U_i \to I_i$ are reduced by 20% compared to the test before for all $k \in \{0,1,2\}$. This may be achieved by additional intervention policies such as lock down. Hereby, the number of infections as well as the number of casualties can be significantly reduced, as shown in Fig. 11 and 12 – this result shows that one should not only rely on vaccination to mitigate the epidemic fast, i.e., the vaccination strategy and intervention policies should be optimized at the same time.

4.4 Effectiveness of the Vaccine

In the last test, a lower effectiveness of the vaccine (compared to before) is investigated. By assuming that the effectiveness is $\chi_i := 0.5\psi_i$ instead of $\chi_i := 0.11\psi_i$, $i \in N$, the outcome from solving Problem 1 is shown in Fig. 13 and 14. As could be expected, this change will lead to less healed cases at the end of the horizon, as well as an increase of casualties.

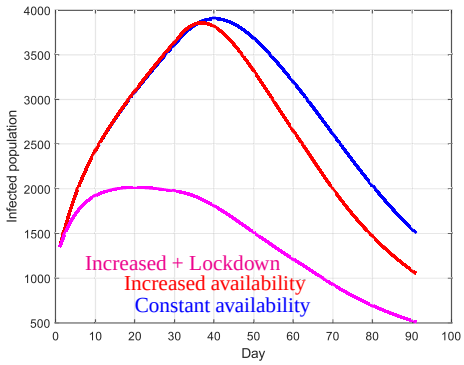

Figure 11: Infections over all age-groups when: 1.) the availability of vaccine is constant over time; 2.) the amount of vaccine increases over the steps; 3.) additional intervention policies are deployed and the amount of vaccine increases over k.

5 CONCLUSION

In this paper, the known SIDARTHE model has been extended in different respects in order to be tailored to the study of vaccination procedure against epidemic virus spread. The motivation of these extensions is the typical shortage of vaccine, if a new virus spreads and the vaccine first has to be developed. To effectively combat the epidemic with a limited amount of vaccine, this paper has shown that the solution of optimal control problems serves to determine strategies to optimally distribute the vaccine among different age-groups. The contacts between the age-groups, heterogeneous infection and mortality rates over the groups, as well as limited effectiveness of the vaccine can all be taken into account in the optimization. The model proposed here can also be adapted straightforwardly to study some additional problems occurring during vaccination procedures, such as the effect that a vac-

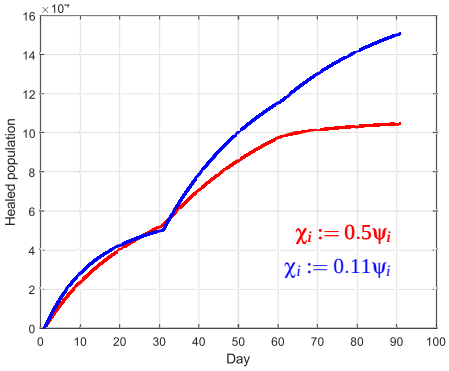

Figure 13: Number of healed persons of all age-groups for different effectiveness of the vaccine.

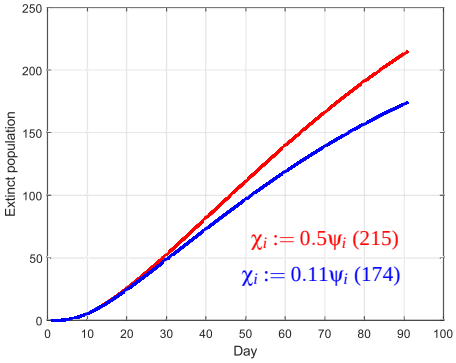

Figure 14: A less effective vaccine leads to an increase of the total number of casualties.

cine is less effective or bears danger for certain age groups, or that a vaccinated person would not get ill but may still be contagious in case of infection.

Finally, for the situation that the transition rates or model parameters are only known within certain intervals, the optimal control problem could be modified into one of optimization under uncertainty, e.g. adopting techniques of robust optimal control. To account for the change of the parameters over time (e.g. due to a virus mutation), the solution of the optimal control problem could be recursively solved over time, leading to a strategy of model predictive control.

REFERENCES

Bock, H., Diehl, M., Leineweber, D., and Schlöder, J. (2000). A direct multiple shooting method for real-time optimization of nonlinear DAE processes. In *Nonlinear model predictive control*, pages 245–267. Springer.

Campo, P. and Morari, M. (1987). Robust model predictive control. In *American control conf.*, pages 1021–1026. IEEE.

Chaturvedi, D. and Chakravarty, U. (2021). Predictive analysis of COVID-19 eradication with vaccination in India, Brazil, and USA. *Infection, Genetics and Evolution*, 92:104834.

Cohen, R., Havlin, S., and Ben-Avraham, D. (2003). Efficient immunization strategies for computer networks and populations. *Physical review letters*, 91(24):247901.

Della, F., Salzano, D., Di Meglio, A., De Lellis, F., Coraggio, M., Calabrese, C., Guarino, A., Cardona-Rivera, R., De Lellis, P., Liuzza, D., et al. (2020). A network model of Italy shows that intermittent regional strategies can alleviate the COVID-19 epidemic. *Nature communications*, 11(1):1–9.

Ganesh, A., Massoulié, L., and Towsley, D. (2005). The effect of network topology on the spread of epidemics. In *24th Joint IEEE Conf. of the Computer and Communications Societies.*, volume 2, pages 1455–1466.

Giordano, G., Blanchini, F., Bruno, R., Colaneri, P., Di Filippo, A., Di Matteo, A., and Colaneri, M. (2020). Modelling the COVID-19 epidemic and implementation of population-wide interventions in Italy. *Nature Medicine*, pages 1–6.

Gourdin, E., Omic, J., and Van Mieghem, P. (2011). Optimization of network protection against virus spread. In *8th Int. IEEE Workshop on the Design of Reliable Communication Networks*, pages 86–93.

Kermack, W. and McKendrick, A. (1932). Contributions to the mathematical theory of epidemics. ii.—the problem of endemicity. *Proc. of the Royal Society of London. Series A*, 138(834):55–83.

Köhler, J., Schwenkel, L., Koch, A., Berberich, J., Pauli, P., and Allgöwer, F. (2020). Robust and optimal predictive control of the COVID-19 outbreak. *Annual Reviews in Control*.

Liu, Z., Lai, Y., and Ye, N. (2003). Propagation and immunization of infection on general networks with both homogeneous and heterogeneous components. *Physical Review E*, 67(3):031911.

López, L. and Rodó, X. (2020). The end of social confinement and COVID-19 re-emergence risk. *Nature Human Behaviour*, 4(7):746–755.

Ndaïrou, F., Area, I., Nieto, J., Silva, C., and Torres, D. (2021). Fractional model of COVID-19 applied to Galicia, Spain and Portugal. *Chaos, Solitons & Fractals*, page 110652.

Pastor-Satorras, R., Vespignani, A., et al. (2003). Epidemics and immunization in scale-free networks. *Handbook of Graphs and Networks, Wiley-VCH, Berlin*.

Peng, C., Jin, X., and Shi, M. (2010). Epidemic threshold and immunization on generalized networks. *Physica A: Statistical Mechanics and its Applications*, 389(3):549–560.

Preciado, V., Zargham, M., Enyioha, C., Jadbabaie, A., and Pappas, G. (2013). Optimal vaccine allocation to control epidemic outbreaks in arbitrary networks. In *52nd IEEE Conf. on Decision and Control*, pages 7486–7491.

Wan, Y., Roy, S., and Saberi, A. (2007). Network design problems for controlling virus spread. In *46th IEEE Conf. on Decision and Control*, pages 3925–3932.

Zanette, D. and Kuperman, M. (2002). Effects of immunization in small-world epidemics. *Physica A: Statistical Mechanics and its Applications*, 309(3-4):445–452.